ResearchGate

See discussions, stats, and author profiles for this publication at: https://www.researchgate.net/publication/6874776

Adsorbed U(VI) Surface Species on Muscovite Identified by Laser Fluorescence Spectroscopy and Transmission Electron Microscopy

ARTICLE *in* ENVIRONMENTAL SCIENCE AND TECHNOLOGY · SEPTEMBER 2006

Impact Factor: 5.33 · DOI: 10.1021/es052507l · Source: PubMed

CITATIONS
33

READS
38

6 AUTHORS, INCLUDING:

Gerhard Geipel
Helmholtz-Zentrum Dresden-Rossendorf
144 PUBLICATIONS **2,555** CITATIONS
SEE PROFILE

R. C. Ewing
Stanford University
796 PUBLICATIONS **16,592** CITATIONS
SEE PROFILE

Available from: R. C. Ewing
Retrieved on: 01 February 2016

Environ. Sci. Technol. **2006**, *40,* 4646−4652

Adsorbed U(VI) Surface Species on Muscovite Identified by Laser Fluorescence Spectroscopy and Transmission Electron Microscopy

THURO ARNOLD,*,† SATOSHI UTSUNOMIYA,‡ GERHARD GEIPEL,† RODNEY C. EWING,‡ NILS BAUMANN,† AND VINZENZ BRENDLER†

FZ Rossendorf e. V., Institute of Radiochemistry, P.O. Box 510119, D-01314 Dresden, Germany, and Department of Geological Sciences, University of Michigan, Ann Arbor, Michigan 48109-1063

Time-resolved laser-induced fluorescence spectroscopy (TRLFS) and high-angle annular dark-field scanning transmission electron microscopy (HAADF−STEM) were applied to investigate the species of uranyl(VI) adsorbed onto muscovite platelets and muscovite suspensions (grain size: 63−200 μm). TRLFS provided evidence for the presence of two adsorbed uranium(VI) surface species on edge-surfaces of muscovite. The two species showed different positions of the fluorescence emission bands and different fluorescence lifetimes indicating a different coordination environment for the two species. HAADF−STEM revealed that nanoclusters of an amorphous uranium phase were attached to the edge-surfaces of muscovite powder during batch sorption experiments. These U-nanoclusters were not observed on {00*l*} cleavage planes of the muscovite. The surface species with the shorter fluorescence lifetimes are interpreted as truly adsorbed bidentate surface complexes, in which the U(VI) binds to aluminol groups of edge-surfaces. The surface species with the longer fluorescence lifetimes are interpreted to be an amorphous U(VI) condensate or nanosized clusters of polynuclear uranyl(VI) surface species with a particle diameter of 1 to 2 nm. Depending on the size of these clusters the fluorescence lifetimes vary; i.e., the larger the nanosized clusters, the longer is the fluorescence lifetime.

Introduction

Uranium migration in natural aqueous systems adjacent to contaminated sites (e.g., mining and milling sites) is an ongoing concern in environmental research. In oxidizing aqueous systems uranium predominantly occurs in the hexavalent oxidizing state (*1*) as the uranyl ion, UO_2^{2+}. Assessing its transport behavior requires a fundamental understanding of the immobilization processes occurring on a molecular scale at mineral−water interfaces. In soils, sediments, and rocks, sorption to silicate minerals contributes significantly to uranium retardation (*2*−*4*). Muscovite, a dioctahedral 2:1 phyllosilicate (ideally $KAl_2[Si_3AlO_{10}](OH)_2$), is a common rock-forming mineral and major constituent of granite and phyllite and thus a potentially important sorbent of uranium. Its structural properties and weathering behavior are extensively described in Fanning et al. (*5*). Micas tend to grow and dissolve along their edge-surfaces (*6*), and these surfaces are also much more reactive for adsorption reactions. In principle, there are three possible binding sites for heavy metals on muscovite: (1) adsorption to the basal plane surface through equatorial coordination of the heavy metal with two adjacent surface oxygen atoms from a siloxane [SiO_4] tetrahedron, (2) cation exchange for interlayer potassium, and (3) adsorption onto the aluminol groups in octahedral coordination of the muscovite edge-surfaces.

The sorption of uranium(VI) on muscovite has been studied using the Freundlich adsorption isotherm (*7*) and the diffuse double layer model (*8*). In the latter the formation of two surface species, a dominant mononuclear bidentate surface complex, $\equiv XO_2UO_2$ and to a minor extent a mononuclear, monodentate surface species, $-XOUO_2^+$ was suggested. However, their spectroscopic evidence was not provided. Polymerization of uranium species and formation of $U^{4+}-U^{5+}-U^{6+}$ linkages on edge-surfaces of ferrous mica by heterogeneous reduction has been observed (*9*) using high-resolution X-ray photoelectron spectroscopy and high-resolution transmission electron microscopy (HRTEM). Since ferrous iron is often an isomorphous replacement in muscovite for octahedral Al (*10*) it may induce similar redox reactions leading to uranium aggregates on muscovite.

No polymeric surface complexes were observed in an X-ray absorption fine structure (XAFS) study about the U(VI) adsorption onto montmorillonite (*11*). The edge surfaces of montmorillonite are similar to the edges of muscovite with respect to the nature of their surface groups. Both are dominated by aluminol groups. Catalano and Brown (*11*) found that in air atmosphere uranyl bound to edge sites occurs as uranyl−carbonato ternary surface complexes. Another XAFS investigation conducted by Moyes et al. (*12*), who studied the U(VI) uptake on muscovite, indicated that uranium sorption on muscovite may occur on basal plane surfaces through surface precipitation.

TRLFS has been increasingly used to study the uranium(VI) adsorption onto silica (*13*), albite (*14*), alumina (*15*), calcite (*16*, *17*), gibbsite (*18*), and smectites (*19*−*21*). TRLFS gives information on the lifetime and spectral characteristics of species (*20*, *22*−*25*), which provides information on the type and number of distinct species.

Recently conducted studies showed that adsorption at near neutral pH conditions occurs predominantly on the edge-surfaces of phyllosilicates (*26*, *27*). However, it is still debated as to whether uranyl species adsorb onto muscovite preferentially on the silanol or aluminol edge sites. Also the number of adsorbed uranyl surface species formed during sorption experiments onto muscovite is not known. In this study we used spectroscopic and microscopic techniques in a complementary fashion, i.e., TRLFS in combination with HAADF−STEM, to address these points and investigate sorbed U(VI) species on muscovite in the pH range 6.5−7 where uranium sorption reaches its maximum. HAADF−STEM has successfully characterized heavy elements in environmental and geological samples at the nano to near atomic scale (*28*−*30*).

Experimental Section

Sorption Experiments with Muscovite Platelets. Muscovite platelets of approximately 1 cm^2 and 5 mm thick were immersed in 0.01 M $NaClO_4$ solution, and the pH was adjusted

* Corresponding author e-mail: T.Arnold@fz-rossendorf.de; phone: +49 (351) 2602432; fax: +49 (351) 2603553.
† FZ Rossendorf e. V., Institute of Radiochemistry.
‡ University of Michigan.

10.1021/es052507l CCC: $33.50
© 2006 American Chemical Society
Published on Web 06/30/2006

to 7.0 using $HClO_4$ and NaOH (0.1 and 0.01 M, respectively) while continuously stirring. At this pH a maximum of uranium(VI) sorption had been previously reported (*2*). All samples were in equilibrium with atmospheric CO_2. The specific surface area was measured by the BET method (Kr, five point adsorption isotherm) to be 0.06 $m^2/g \pm 10\%$. The sorption experiment was then conducted following the procedure described in Ames et al. (*7*). The pH was readjusted each day until it was stable. At this point, a uranyl(VI) stock solution (pH 1.5, 0.01 M $NaClO_4$) was added to achieve a total uranium(VI) concentration of 1×10^{-5} M, and the pH value was immediately readjusted to 7.0. A contact time of 60 h ensured complete uranium(VI) sorption. Then the final pH was measured, and the uranium concentration in solution was determined by ICP-MS (ELAN 5000 and ELAN 6000, Perkin-Elmer). After centrifugation, the vials (made of polypropylene) were emptied and rinsed with deionized water. To remove uranium from the container walls 40 mL 1 M HNO_3 was added, and the vials were again placed in the overhead mixer for another 24 h and subsequently analyzed for desorbed uranium by ICP-MS. With the obtained uranium contents in solution and on the container walls, the total amount of sorbed uranium was calculated; 72.6% ± 5% of the initially added U(VI) was adsorbed.

Time-Resolved Laser-Induced Fluorescence Spectroscopy (TRLFS). TRLFS spectra were collected in situ in solution, on basal plane surfaces and edge-surfaces of the muscovite platelets. Just prior to the measurement, the samples were thoroughly rinsed with deionized water to remove any aqueous uranium species. Throughout the TRLFS measurements of approximately 20−30 min, the samples were covered with a water film that persisted for the time of analysis. The TRLFS system consists of a Nd:YAG diode laser with subsequent fourth harmonic generation. This wavelength (266 nm) was used for the excitation of the samples. The emitted fluorescence radiation was focused into a spectrograph (270M, Jobin Yvon Spec., from 407 to 635 nm) and the resulting spectra were measured by a diode array (701 intensified diodes). The gate width (exposure time) was set to 5 μs. The delay time after the excitation laser pulse ranged from 30 to 6500 ns. For further details concerning the setup of the TRLFS equipment and operation modes, see Geipel et al. (*31*). Every spectrum was measured three times, and for each spectrum, 100 laser shots were averaged. Thirty-one spectra, at steadily increasing delay times, were collected for a single time-resolved spectrum. The evaluation of the spectroscopic data was performed with in-house software by Brendler et al. (32) to obtain the fluorescence lifetimes and the single component spectra. The peak deconvolution of the latter and the generation of all graphics utilized the Origin 6.01 software (OriginLab Corp., Northampton, MA). To constrain the peak deconvolution process, the first emission peak was set to 4.6% of the overall fluorescence intensity, which is in accordance to results published by Bell and Biggers (*33*). For all peak maximum positions the fitting procedure was confined by upper and lower limits for the full-width half-maximum (fwhm) as specified in the Supporting Information. On the basis of the fluorescence spectra at different delay times, the fluorescence decay function was determined. For each single wavelength, the respective fluorescence decay curve was fitted to a sum of exponential decay terms. The lifetimes were averaged over all wavelengths, weighted by their standard deviation. A bi-exponential decay function $y = y_0 + A_1 e^{-(x-x_0)/t_1} + A_2 e^{-(x-x_0)/t_2}$ yielding two fluorescence decay times gave the best approximation. In all cases, assuming only a mono-exponential decay resulted in significantly worse fittings; whereas three-exponential decay functions either did not converge or yielded an unacceptably large scatter in the lifetimes. All spectra were corrected for the laser dispersion peak at 532 nm. For the calculation of the mean lifetime this section of the spectrum (532 ± 4 nm) was excluded.

Transmission Electron Microscopy (TEM), TRLFS, and Sorption Experiments with Muscovite Powders. Since muscovite platelets breaks parallel to their cleavage planes during the cutting and polishing step, considerable contamination penetrated into their interlayers, and thus it was not possible to obtain useful TEM specimens. To overcome this problem, additional batch sorption experiments were conducted with 1×10^{-5} M U(VI) sorbing onto muscovite powder (grain size fraction 63−200 μm). These experiments were completed in 0.01 M $NaClO_4$ media at pH 6.5 using a solid concentration of 12.5 g/L. All samples were in equilibrium with atmospheric CO_2. After crushing the muscovite samples, tiny particles attached on the grains were thoroughly removed by repeated settling and ultrasonic cleaning in acetone. This ultrasonic treatment was applied for 3−5 min, and the procedure was repeated 5 times. The acetone was changed after every cleaning step. The specific surface area of the ultrasonically cleaned muscovite was 0.31 $m^2/g \pm 10\%$ determined with the BET method (N_2, five point adsorption isotherm). Its chemical composition is provided in the Supporting Information. Prior to the addition of uranium, the pH of the muscovite suspension was adjusted to pH 6.5 and readjusted every second day using again NaOH and $HClO_4$ until the pH became stable. The addition was performed while continuously stirring the samples. Then uranium, using the stock solution as described above, was added to give a total uranium concentration in the respective samples of 1×10^{-5} M U(VI). A contact time of 3 days was applied to ensure that the sorption process was completed. Then the muscovite suspension were centrifuged at 67 500*g* for 1 h and a sample of the supernatant was taken to determine the uranium concentration in solution. After that the centrifuged sample was decanted and subsequently washed with a solution of identical pH and ionic strength. Afterward aliquots of the suspensions were used for additional TRLFS measurements. Uranium sorption onto container walls was accounted for as described before. It was found that 70.5% ± 5% of the initially added U(VI) was adsorbed. The TRLFS measurements were conducted while stirring the sample to avoid settling of the muscovite particles during the TRLFS measurements. The remaining suspensions were again decanted and dried at 40 °C. The dry powder of muscovite was dispersed on a holey carbon mesh of TEM Cu-grid. The TEM analysis was employed using a JEOL 2010F with field-emission gun equipped with energy-dispersive X-ray analysis (EDX) at the Electron Microprobe Analysis Laboratory (EMAL) of the University of Michigan. The system is controlled by FasTEM. The spherical aberration coefficient is 1.0 mm. The spatial resolution is 0.25 nm. The probe size in STEM mode was 0.2 nm for high-resolution imaging and 0.5 nm for EDX analysis. The inner angle of the HAADF detector was 50 mrad. In general, an image contrast in HAADF−STEM is correlated to the atomic mass: heavier elements contribute to brighter contrast (*34*). A detailed procedure of HAADF−STEM was described in Utsunomiya and Ewing (*34*).

Results

TRLFS on Muscovite Platelets. The fluorescence of the uranium(VI) species carries two types of characteristic information: the position of the fluorescence emission bands and the fluorescence lifetime (*35*). Here the positions of the fluorescence emission bands are primary features of the TRLFS spectrum, whereas the fluorescence lifetime is secondary, because it is dependent on the sample preparation (wet or dry) and the temperature of the experiment (*36*). The fluorescence lifetime varies because of diffusional quenching effects depending on the number of neighboring water

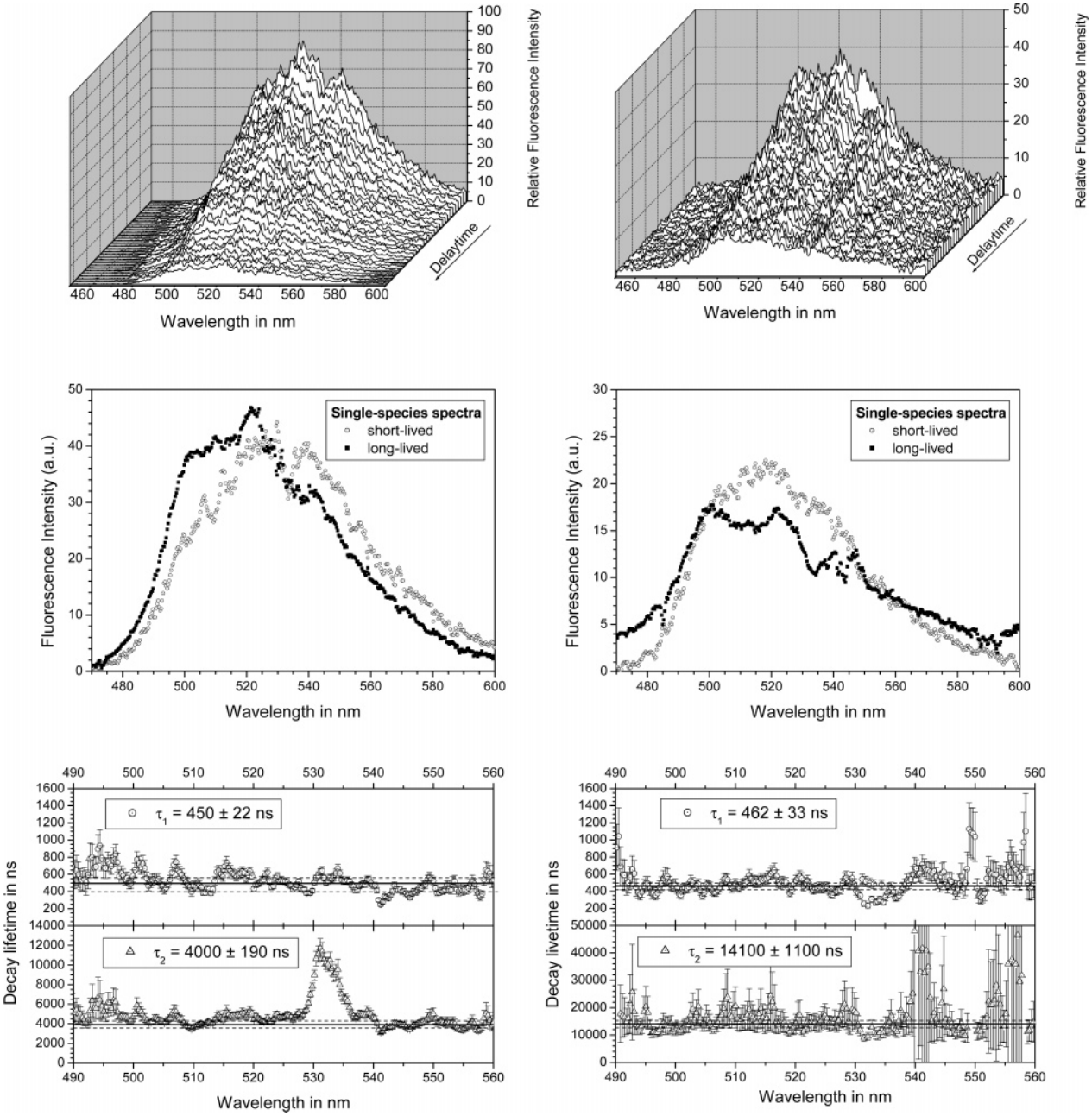

FIGURE 1. Top: TRLFS spectra; middle: convoluted single spectra at $t = 0$; bottom: fluorescence decay lifetime as function of the wavelength, error bars correspond to 2 σ. Left side: U(VI) sorption onto muscovite edge-surfaces, TRLFS evaluation at pH 7.0. Right side: U(VI) sorption on muscovite suspensions, TRLFS evaluation at pH 6.5. Both spectra were corrected for the laser dispersion peak at 532 nm as stated in the Experimental Section. This procedure worked better for suspension than for the platelets. Therefore the remnant of this laser peak is still present in the spectrum seemingly increasing the lifetime of the long-lived species. For the calculation of the mean lifetime this section of the spectrum (532 ± 4 nm) was excluded.

molecules surrounding the uranium(VI) atom (*37*). Such characteristic spectral information is useful for the identification of fluorescent aqueous uranium species, as well as uranyl(VI) surface species adsorbed onto minerals.

TRLFS of the solution, in which the platelets were immersed, showed a spectra with very low intensity typical for the remaining U(VI) concentration in solution. The spectra of the basal plane surfaces of muscovite showed no U(VI) fluorescence signal at all, clearly indicating that U(VI) does not significantly adsorb onto basal plane surfaces. However, a strong fluorescence signal was obtained from the edge surfaces showing that U(VI) adsorption occurs predominantly onto edge-surfaces. These results are not consistent with results published by Moyes et al. (*12*). They found that uranium uptake on muscovite may occur on basal plane surfaces through surface precipitation in which the first layer of uranium atoms binds through equatorial coordination of two adjacent surface oxygens from a silicate tetrahedron, with the axial oxygens of the uranyl unit aligned across the hexagonal cavities created by the rings of tetrahedra. However, they used a uranium(VI) concentration well above the solubility limits of common uranium(VI) phases, which is not appropriate for obtaining information about adsorbed U species.

The deconvoluted TRLF spectra of the adsorbed U(VI) surface species on muscovite edges indicated two surface species with different fluorescence lifetimes. The fluorescence emission spectra of both species are shown in Figure 1. The first species has a fluorescence lifetime of 450 ± 22 ns, and the second species has a distinctively larger one of 4000 ±

TABLE 1. Lifetimes and Emissions Bands of the Two U(VI) Surface Species[a]

species	lifetimes [ns]	fluorescence emission bands					
		species detected on the edge-surfaces of muscovite platelets					
1	450 ± 22	491.4 ± 2.2 (21.2)	504.2 ± 1.0 (16.4)	521.5 ± 0.9 (12.2)	541.6 ± 1.2 (8.9)	563.0 ± 4.3 (4.9)	588.7 ± 4.7 (3.2)
2	4000 ± 190	487.8 ± 1.4 (17.6)	501.7 ± 0.5 (13.9)	519.4 ± 0.7 (10.1)	538.8 ± 1.4 (6.1)	558.8 ± 5.6 (0.7)	583.6 ± 6.3 (−1.9)
		species detected in suspension					
1	462 ± 33	488.4 ± 3.2 (18.2)	500.9 ± 1.0 (13.1)	517.0 ± 1.2 (7.7)	536.1 ± 1.8 (3.4)	557.7 ± 6.3 (−0.4)	582.3 ± 9.3 (−3.2)
2	14100 ± 1100	484.5 ± 1.7 (14.3)	499.7 ± 0.6 (11.9)	519.2 ± 0.5 (9.9)	541.1 ± 1.5 (8.4)	558.6 ± 3.7 (0.5)	573.4 ± 24 (−12.1)

[a] In parentheses: Observed shift with respect to uranyl(VI) in $NaClO_4$. Errors associated with the peak positions are 2σ.

190 ns. Six fluorescence emission bands as reported by Bell and Biggers (*38*) were used to describe the TRLFS spectra. The results for the adsorbed U(VI) species on muscovite edges are summarized in Table 1a. For the discussion only the first 5 peaks were considered, since the sixth emission band is very small and therefore very uncertain. The maxima are shifted significantly relative to the values for the free uranyl ion in perchlorate medium (*38*). The shifts range from 21 nm for the first maxima (short-lived) and decrease to 1 (long-lived) and 5 nm (short-lived) for the fifth ones, respectively (Table 1a). The first three fluorescence emission bands of both U(VI) surface species are significantly shifted to higher wavelengths as compared with the aqueous $(UO_2)_3(OH)_5^+$ (*39*) complex, typical for the applied experimental conditions. The only other relevant aqueous U(VI) species, $(UO_2)_2CO_3(OH)_3^-$, does not show any fluorescence at room temperature (*40*). We suggest to attribute the acquired fluorescence signals to adsorbed U(VI) surface species and not to aqueous U(VI) complexes.

Due to the pronounced shift to higher wavelengths (2 to 5 nm) of all the fluorescence peaks of the short-lived species in relation to the long-lived species, it is assumed that the two adsorbed uranium(VI) edge-surface species on muscovite differ in their coordination environment. Namely, they should have different numbers of hydroxyl groups in their first coordination sphere, as different numbers of hydroxyl groups cause changes in the spectral features (*24*). Also the different lifetimes indicate a different number of quenchers, very likely water molecules that surround the attached uranium surface species.

TRLFS on Muscovite Suspensions in Contact with Uranium. The deconvoluted TRLF spectra of the adsorbed U(VI) surface species on muscovite suspensions again indicated two surface species with different fluorescence lifetimes and different positions of the emission bands. The fluorescence emission spectra, the deconvoluted spectra, and the lifetime determinations of both species are shown in Figure 1. The first species has a fluorescence lifetime of 462 ± 33 ns, and the second species a distinctively larger one of 14 100 ± 1100 ns, for further details see Table 1b. Based on the TRLFS results obtained for the platelets, it is assumed that the adsorption occurs exclusively on the edge-surfaces of the muscovite grains. Again the maxima are significantly shifted relative to the values for the free uranyl ion in perchlorate medium, and the shifts range from 18 nm for the first maxima to approximately zero for the fifth ones. In contrast to the platelets, no pronounced shift to higher wavelengths of all the fluorescence peaks of the short-lived species in relation to the long-lived species was observed here. Comparing the adsorbed U(VI) surface species on the muscovite edges with the ones in suspension, it was found that there were slight differences in the positions of the peak maxima. At this stage it not clear if these observations should be attributed to poor counting statistics, or if they truly represent differences in the coordination environment of U(VI). Comparing the lifetime of the short-lived species on the edges and in suspension, we found good agreement within the errors of the measurements. However, the fluorescence lifetime of the long-lived species on the edges and in suspension differ from each other. These differences are attributed to a different number of water molecules surrounding the attached uranium surface species.

There is also a difference in the intensity ratio $I_{\text{short-lived}}/I_{\text{long-lived}}$ of the adsorbed uranium species on muscovite edge-surfaces and muscovite suspensions. On the edges we calculated a ratio of 0.99, and for the suspensions we obtained a ratio of 1.54. From this we conclude that relatively more long-lived uranium surface species are sorbed onto the edges of the muscovite platelets than on the edge-surfaces of the muscovite suspension.

TEM Observation. TEM measurements reveal that after searching the entire region of the muscovite platelets (63−200 μm grain size) no uranium was observed on the basal plane of muscovite, confirming the TRLFS results. On the edge-surfaces, however, uranium was detected by HAADF−STEM. The HAADF−STEM image (Figure 2a) showed a few nanometer-sized clusters with bright contrast, for which semiquantitative EDX analyses revealed a few wt % of U. Because the EDX analysis included the signal from the underlying muscovite as Figure 2b reveals high Si and Al peaks in the spectrum, the actual concentration of U in the cluster is much higher than a few wt %. It was difficult to obtain an distinct peak for K because the K-line of potassium overlaps the M-line of uranium in the EDX analysis. The U-rich clusters occurred ubiquitously at the edge of muscovite. An electron diffraction pattern selecting the area where several U-rich clusters were present did not show any diffraction maxima except for the pattern of muscovite, indicating that the particles are not crystalline, but amorphous. Probably these clusters or nanoparticles are "polymerized" U (oxy-)hydroxyls in a size range of 1−2 nm.

Elemental maps of the area containing several U-rich clusters show that a correlation among Al, Si, and U is not conclusive, because the Al concentration is so high. However, some of the U-distributions as shown in Figure 3 are correlated with Fe distributions. A few Fe nanoparticles were also found at the muscovite edges associated with some U-distributions. This might indicate that the U-rich particles can also associate with Fe-particles and form aggregates at the nanoscale. However, most of the visualized U-clusters were independently distributed from Fe at the edges of the muscovite. Since iron quenches the fluorescence emission of uranium(VI) the two detected fluorescence signals on the muscovite edge surfaces cannot be attributed to uranium−iron agglomerates. Additionally conducted batch sorption experiments using a total uranium concentration of 2×10^{-6} M and associated HAADF−STEM investigations showed no uranium nanoparticles indicating that neither U nanopar-

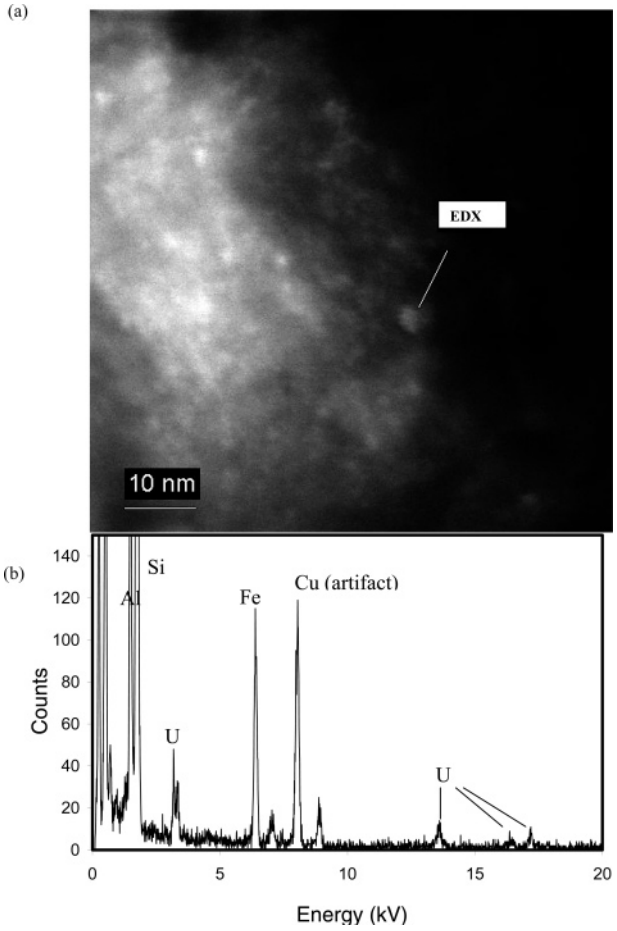

FIGURE 2. (a) HAADF−STEM images of uranium nanoparticles on muscovite edge-surfaces. (b) EDX spectrum of uranium nanoparticles—bright dots shown in HAADF−STEM image, see (a)—on muscovite edge-surfaces. EDX profile. Trace amounts (a few wt %) of uranium were detected.

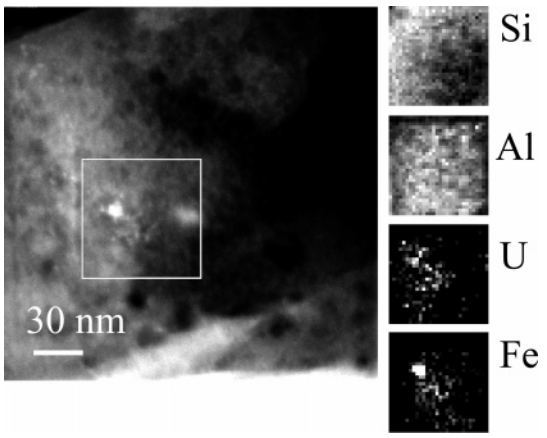

FIGURE 3. HAADF−STEM image showing an elemental mapping around U-rich clusters. A correlation among Al, Si, and U is not conclusive, since the Al concentration is so high. Some of the U-distributions as shown in this picture are correlated with Fe distributions. However, most of the visualized U-phases were independently distributed from Fe at the edges of the muscovite.

ticles nor U−Fe aggregates did exist on the muscovite edges prior to the U(VI) sorption experiments. Besides the formation of truly adsorbed surface complexes there might be an additional mechanism for the formation of U-nanoparticles on muscovite edge surfaces. This possible mechanism could be related to defects in the substrate surface which may provide sites of nucleation and eventually grow and form U-nanoparticles.

Discussion

Self-assembling nanospheres from actinide ions and their persistence as stable entities in alkaline solutions is described by Burns et al. (*41*). Such nanospheres have compositions of, e.g., $[K_{16}(H_2O)_2(UO_2)(O_2)_2(H_2O)_2\{(UO_2)(O_2)_{1.5}\}_{28}]^{14-}$ and are likely present in natural and contaminated samples (*41*). They could explain our observation of uranium nanoparticles on the edges of muscovite. The muscovite used in our study contains structural Fe^{2+} as isomorphous replacement for Al. Heterogeneous reduction of uranium and simultaneous oxidation of ferrous iron as described by Ilton et al. (*9*) of aqueous U(VI) at mica edge surfaces may possibly induce the formation of some U-nanoparticles on muscovite edges. However, it is not clear to what extent and if these would be detectable by TRLFS and HAADF−STEM analyses.

Based on TRLFS and HAADF−STEM investigations we found two U(VI) species and were able to visualize uranium nanoparticles. By using an excitation wavelength of 266 nm, only U(VI) species will be fluorescent and therefore can be detected by TRLFS. It does not detect, if present or not, nonfluorescent U(VI) carbonates, or U(IV) and U(V) species. However, such surface species may also be present. HAADF−STEM investigations revealed the presence of uranium nanoparticles, but not the oxidation state therein. It is highly likely that the detected uranium nanoparticles contained U(VI), since U(VI) was detected by TRLFS. However, currently the presence of U(V) and U(IV) contribution cannot be ruled out. Considering the composition of the aqueous bulk solution (see Supporting Information) in contact with the muscovite, the phases that are most likely to form are compreignacite, soddyite, and schoepite. However, these phases are not supersaturated as EQ3/6 calculations indicate by using solubility products of Guillaumont et al. (*42*).

Thompson et al. (*43*) used XAFS to study U(VI) sorption onto kaolinite under experimental conditions similar to the conditions of this study. They reported that in the pH range from 6 to 7 in the presence of air, mononuclear uranyl species dominate; whereas, from pH 7 to 7.9 in air multinuclear U species were dominant. Such multinuclear sorbates could be precursors of U surface precipitates forming uranium nanoparticles. The adsorption of uranium(VI) on γ-alumina surfaces was studied at pH 6.5 by Sylwester et al. (*27*) also using XAFS spectroscopy. They found a splitting of the uranyl-(VI) equatorial coordination sphere of oxygens and interpreted this as the formation of mononuclear inner-sphere surface complexes. In addition they also reported a uranium shell at 4.01 C with a coordination number of 0.43 and explained it as some evidence of the partial formation of polynuclear uranyl complexes along with mononuclear complexes. Two adsorbed uranyl(VI) surface species on gibbsite with fluorescence lifetimes of 330 ns and 5600 ns were identified by Baumann et al. (*18*) using TRLFS. They attributed the short-lived species to a bidentate mononuclear inner-sphere surface complex and the longer-lived species to small clusters consisting of sorbed polynuclear surface species. However, their postulated sorbed polynuclear U(VI) clusters were not verified by electron microscopy.

Two uranyl surface species on smectite edge sites were reported by Chisholm-Brause et al. (*19*) using time-resolved optical emission spectroscopy and uranyl wet paste samples. At pH 4.1−5.5 only one species, interpreted as a monomeric species, was detected. By raising the pH a second surface species shifted by 155 cm^{-1} to lower energy values appeared and with increasing the pH gradually up to 8.1 this species became more and more important. It was interpreted as a more hydrolyzed uranyl surface complex, e.g., $(UO_2)_3(OH)_5^+$). Based on its longer lifetime it was assigned to a hydrolyzed

species on a silanol site, since, as the authors argue, the lifetime of the hydrolyzed species on an >AlO^- site should remain approximately equal to the lifetime of a monomeric species on an >AlO^- site. We disagree with this interpretation, since it cannot be expected that two different surface species with different coordination environments have identical lifetimes.

Shorter fluorescence lifetimes indicate more water molecules in the coordination environment of the respective adsorbed uranium(VI) surface species, because water molecules quench the fluorescence lifetime. On this basis and in analogy to the interpretation of Baumann et al. (*18*) the obtained results are interpreted in the following way. The surface species with the shorter fluorescence lifetimes (edges of platelets 450 ± 22 ns; suspensions 462 ± 33 ns) are regarded as truly adsorbed bidentate surface complexes, in which two equatorial oxygen atoms of the free uranyl(VI) moiety bind to two aluminol binding sites of the muscovite edge-surface and form an inner-sphere bidentate surface complex. This is similar to the uranyl(VI) adsorption process described by Hennig et al. (*26*) on montmorillonite and Sylwester et al. (*27*) on silica, alumina, and montmorillonite. In contrast, Catalano and Brown (*11*) found that uranyl bound to montmorillonite edge sites occurs as uranyl−carbonato ternary surface complexes in systems equilibrated with atmospheric CO_2. Such uranyl−carbonato ternary surface complexes are not detectable by TRLFS, since carbonate usually quenches the fluorescence signal of U(VI) at room temperature (*40*). Only in cases where Ca is a constituent of the U(VI) species can TRLFS spectra be detected (*44*), but Ca is not present in our sample. Nevertheless, the presence of adsorbed uranyl−carbonato ternary surface complexes on muscovite cannot be ruled out.

The surface species with the distinctively longer fluorescence lifetimes of 4000 ± 190 ns on edges of muscovite platelets and for the muscovite suspension of 14 100 ± 1100 ns are interpreted as an amorphous U(VI) condensate or nanosized clusters of polynuclear uranyl(VI) surface species with a particle diameter of 1−2 nm. The size of the polynuclear uranyl surface species correlates with the fluorescence lifetime (*24*, *45*), i.e., the larger the nanosized particles, the longer the fluorescence lifetime. In this context the longer fluorescence lifetimes of the long-lived U(VI) surface species on the edges of muscovite platelets are interpreted as larger particles than the ones found on edge-surfaces of the smaller muscovite grains (63−200 μm).

The precipitation of nanosized uranyl(VI) clusters that form during sorption experiments of uranyl(VI) with mineral surfaces seems to be a process that has been generally overlooked. However, to better describe and model sorption experiments, the precipitation of solid uranyl(VI) phases as nanosized, poorly crystalline particles should also, in addition to surface complexation models, be considered.

Acknowledgments

H. Neubert is thanked for sample preparation, D. Birnstein and C. Eckardt for BET measurements, U. Schaefer for ICP-MS analyses, and U. Schüssler for EMPA analyses. Two anonymous reviewers are thanked for their constructive comments. Financial support through the EU Project ACTAF (Contract FIKW-CT-2000-00035) is also gratefully acknowledged. The work at the University of Michigan (R.C.E. and S.U.) was supported by the Office of Science and Technology and International (OSTI) of the Office of Civilian Radioactive Waste Management (DE-FE28-04RW12254). The views, opinions, findings, and conclusions or recommendations of the authors expressed herein do not necessarily state or reflect those of the DOE/OCRWM/OST&I.

Supporting Information Available

Additional information about the fitting procedure of the TRLFS results; EMPA analyses of ultrasonically cleaned muscovite; and concentrations of Mg, Al, Si, K, Ti, and U in solution at the end of the batch sorption experiments. This material is available free of charge via the Internet at http://pubs.acs.org.

Literature Cited

(1) Grenthe, I.; Fuger, J.; Konings, R. J. M.; Lemire, R. J.; Muller, A. B.; Nguyen-Trung, C.; Wanner, H. *Chemical Thermodynamics of Uranium*. Elsevier: New York, 1992.

(2) Arnold, T.; Zorn, T.; Bernhard, G.; Nitsche, H. Sorption of Uranium(VI) onto Phyllite. *Chem. Geol.* **1998**, *151*, 129−141.

(3) Payne, T. E.; Davis, J. A.; Waite, T. D. Uranium Retention by Weathered Schists − The Role of Iron. *Radiochim. Acta* **1994**, *66*/*67*, 297−303.

(4) Yanase, N.; Nightingale, T.; Payne, T. E.; Duerden, P. Uranium Distribution in Mineral Phases of Rock by Sequential Extraction Procedure. *Radiochim. Acta* **1991**, *52*/*53*, 387−393.

(5) Fanning, D. S.; Keramidas, V. Z.; El-Desoky, M. A. Micas. In *Minerals in Soil Environments*; Dixon, J., Weed, S., Eds.; Soil Science Society of America: Madison, WI, 1989; pp 551−634.

(6) Murakami, T.; Utsunomiya, S.; Yokoyama, T.; Kasama, T. Biotite dissolution process and mechanisms in the laboratory and in nature: Early stage weathering environment and vermiculitization. *Am. Mineral.* **2003**, *88*, 377−386.

(7) Ames, L. L.; McGarrah, J. E.; Walker, B. A. Sorption of Uranium and Radium by Biotite, Muscovite, and Phlogopite. *Clays Clay Miner.* **1983**, *31*, 343−351.

(8) Arnold, T.; Zorn, T.; Zänker, H.; Bernhard, G.; Nitsche, H. Sorption behavior of U(VI) on phyllite: experiments and modeling. *J. Contam. Hydrol.* **2001**, *47*, 219−231.

(9) Ilton, E. S.; Haiduc, A.; Cahill, C. L.; Felmy, A. R. Mica surfaces stabilize pentavalent uranium. *Inorg. Chem.* **2005**, *44* (9), 2986−2988.

(10) Deer, W. A., Howie, R. A., Zussman, J. *An Introduction to the Rock-Forming Minerals*, 2nd ed.; Longman: London, 1992; 696 pp.

(11) Catalano, J. G.; Brown, G. E., Jr. Uranyl adsorption onto montmorillonite: Evaluation of binding sites and carbonate complexation. *Geochim. Cosmochim. Acta* **2005**, *69* (12), 2995−3005.

(12) Moyes, L. N.; Parkman, R. H.; Charnock, J. M.; Vaughan, D. J.; Livens, F. R.; Hughes, C. R.; Braithwaite, A. Uranium Uptake from Aqueous Solution by Interaction with Goethite, Lepidocrocite, Muscovite, and Mackinawite: An X-ray Absorption Spectroscopy Study. *Environ. Sci. Technol.* **2000**, *34* (6), 1062−1068.

(13) Gabriel, U.; Charlet, L.; Schläpfer, C. W.; Vial, J. C.; Brachmann, A.; Geipel, G. Uranyl Surface Speciation on Silica Particles Studied by Time-Resolved Laser-Induced Fluorescence Spectroscopy. *J. Colloid Interface Sci.* **2001**, *239*, 358−368.

(14) Walter, M.; Arnold, T.; Geipel, G.; Scheinost, A.; Bernhard, G. Characterization of the uranium(VI) sorption on albite using TRLFS and EXAFS spectroscopy. *J. Colloid Interface Sci.* **2005**, *282* (2), 293−305.

(15) Kowal-Fouchard, A.; Drot, R.; Simoni, E.; Ehrhardt, J. Use of Spectroscopic Techniques for Uranium(VI)/Montmorillonite Interaction Modeling. *Environ. Sci. Technol.* **2004**, *38*, 1399−1407.

(16) Elzinga, E. J.; Tait, C. D.; Reeder, R. J.; Rector, K. D.; Donohoe, R. J.; Morris, D. E. Spectroscopic investigation of U(VI) sorption at the calcite-water interface. *Geochim. Cosmochim. Acta* **2004**, *68* (11), 2437−2448.

(17) Reeder, R. J.; Nugent, M.; Lamble, G. M.; Tait, C. D.; Morris, D. E. Uranyl incorporation into calcite and aragonite: XAFS and luminescence studies. *Environ. Sci. Technol.* **2000**, *34*, 638−644.

(18) Baumann, N.; Brendler, V.; Arnold, T.; Geipel, G.; Bernhard, G. Uranyl sorption onto gibbsite studied by Time-resolved Laser-induced Fluorescence Spectroscopy (TRLFS). *J. Colloid Interface Sci.* **2005**, *290*, 318−324.

(19) Chisholm-Brause, C. J.; Berg, J. M.; Little, K. M., Matzner, R. A.; Morris, D. E. Uranyl sorption by smectites: spectroscopic assessment of thermodynamic modeling. *J. Colloid Interface Sci.* **2004**, *277*, 366−382.

(20) Chisholm-Brause, C.; Berg, J. M.; Matzner, R. A.; Morris, D. E. Uranium(VI) sorption complexes on montmorillonite as a function of solution chemistry. *J. Colloid Interface Sci.* **2001**, *233*, 38−49.
(21) Morris, D. E.; Chisholm-Brause, C. J.; Barr, M. E.; Conradson, S. D.; Eller, P. A. Optical spectroscopic studies of the sorption of UO_2^{2+} species on a reference smectite. *Geochim. Cosmochim. Acta* **1994**, *58* (17), 3613−3623.
(22) Kato, Y.; Meinrath, G.; Kimura, T.; Yoshida, Z. A Study of U(VI) Hydrolysis and Carbonate Complexation by Time-Ressolved Laser-Induced Fluorescence Spectroscopy (TRLFS). *Radiochim. Acta* **1994**, *64*, 107−111.
(23) Bernhard, G.; Geipel, G.; Brendler, V.; Nitsche, H. Speciation of Uranium in Seepage Waters of a Mine Tailing Pile Studied by Time-Resolved Laser-Induced Fluorescence Spectroscopy (TRLFS). *Radiochim. Acta* **1996**, *74*, 87−91.
(24) Eliet, V.; Bidoglio, G.; Omenetto, N.; Parma, L.; Grenthe, I. Characterisation of Hydroxide Complexes of Uranium(VI) by Time-resolved Fluorescence Spectroscopy. *J. Chem. Soc., Faraday Trans.* **1995**, *91*, 2275−2285.
(25) Moulin, C.; Laszak, I.; Moulin, V.; Tondre, C. Time-resolved laser-induced fluorescence as a unique tool for low-level uranium speciation. *Appl. Spectrosc.* **1998**, *52*, 528−535.
(26) Hennig, C.; Reich, T.; Dähn, R.; Scheidegger, A. M. Structure of uranium sorption complexes at montmorillonite edge sites. *Radiochim. Acta* **2002**, *90*, 653−657.
(27) Sylwester, E. R.; Hudson, E. A.; Allen, P. G. The structure of uranium (VI) complexes on silica, alumina, and montmorillonite. *Geochim. Cosmochim. Acta* **2000**, *64* (14), 2431−2438.
(28) Utsunomiya, S.; Jensen, K. A.; Keeler, G. J.; Ewing, R. C. Uraninite and Fullerene in Atmospheric Particulates. *Environ. Sci. Technol.* **2002**, *36* (23), 4943−4947.
(29) Utsunomiya, S.; Jensen, K. A.; Keeler, G. J.; Ewing, R. C. Direct identification of trace metals in fine and ultrafine particles in the Detroit urban atmosphere. *Environ. Sci. Technol.* **2004**, *38* (8), 2289−2297.
(30) Utsunomiya, S.; Palenik, S.; Valley, J. W.; Cavosie, A. J.; Wilde, S. A.; Ewing, R. C. Nanoscale occurrence of Pb in an Archean zircon. *Geochim. Cosmochim. Acta* **2004**, *68* (22), 4679−4686.
(31) Geipel, G.; Brachmann, A.; Brendler, V.; Bernhard, G.; Nitsche, H. Uranium (VI) Sulfate Complexation studied by Time-Resolved Laser-Induced Fluorescence Spectroscopy (TRLFS). *Radiochim. Acta* **1996**, *75*, 199−204.
(32) Brendler, V.; Brachmann, A.; Geipel, G. Software to compute fluorescence lifetimes from Time-Resolved Laser-Induced Fluorescence Spectroscopy (TRLFS) studies, Exploiting the full spectrum. In *Annual Report 1996*; Report FZR-180; Forschungszentrum: Rossendorf, 1997; p 13.
(33) Bell, J. T.; Biggers, R. E. Absorption Spectrum of the Uranyl ion in Perchlorate Media. *J. Mol. Spectrosc.* **1968**, *25*, 312−328.
(34) Utsunomiya, S.; Ewing, R. C. Application of High-Angle Annular Dark Field Scanning Transmission Electron Microscopy, Scanning Transmission Electron Microscopy-Energy Dispersive X-ray Spectrometry, and Energy-Filtered Transmission Electron Microscopy to the Characterization of Nanoparticles in the Environment. *Environ. Sci. Technol.* **2003**, *37*, 786−791.
(35) Amayri, S.; Arnold, T.; Reich, T.; Foerstendorf, H.; Geipel, G.; Bernhard, G.; Massanek, A. Spectroscopic characterization of the uranium carbonate Andersonite. *Environ. Sci. Technol.* **2004**, *38*, 6032−6036.
(36) Wang, Z.; Zachara, J. M.; Gassman, P. L.; Liu, C.; Catalano, J. *Fluorescence Spectrocopic Studies of Uranium-bearing Vadose Zone Sediments. In Digest of Science and Technology Program Evaluation, Appendix D*; Hanford Vadoze Zone Report; RPP-10098; Pacific Northwest National Laboratory: Richland, WA, 2002.
(37) Geipel, G.; Bernhard, G.; Rutsch, M.; Brendler, V.; Nitsche, H. Spectroscopic properties of uranium(VI) minerals studied by time-resolved laser-induced fluorescence spectroscopy (TRLFS). *Radiochim. Acta* **2000**, *88*, 757−762.
(38) Bell, J. T.; Biggers, R. E. The absorption spectrum of the uranyl ion in perchlorate media. Part I. Mathematical resolution of the overlapping band structure and studies of the environmental effects. *J. Mol. Spectrosc.* **1965**, *18*, 247−275.
(39) Sachs, S.; Brendler, V.; Geipel, G. Uranium(VI) Complexation by Humic Acid under Neutral pH Conditions Studied by Laser-induced Spectroscopy. *Radiochim. Acta*, submitted.
(40) Wang, Z.; Zachara, J. M.; Yantasee, W.; Gassman, P. L.; Liu, C.; Joly, A. G. Cryogenic laser induced fluorescence characterization of U(VI) in Hanford vadose zone pore waters. *Environ. Sci. Technol.* **2004**, *38*, 5591−5597.
(41) Burns, P. C.; Kubatko, K.-A.; Sigmon, G.; Fryer, B. J.; Gagnon, J. E.; Antonio, M. R.; Soderholm, L. Actinyl Peroxide Nanospheres. *Angew. Chem.* **2005**, *117*, 2173−2177.
(42) Guillaumont, R.; Fanghänel, T.; Fuger, J.; Grenthe, I.; Neck, V.; Palmer, D. A.; Rand, M. H. Update on the chemical thermodynamics of uranium, neptunium, plutonium, americium and technetium. In *Chemical Thermodynamics Vol. 5*; OECD Nuclear Energy Agency, Ed.; Elsevier: Amsterdam, 2003.
(43) Thompson, H. A.; Parks, G. A.; Brown, G. E., Jr. Structure and Composition of Uranium(VI) Sorption Complexes at the Kaolinite-Water Interface. In *Adsorption of Metals by Geomedia*; Jenne, E. A., Ed.; Academic Press: San Diego, CA, 1998; pp 349−370.
(44) Bernhard, G.; Geipel, G.; Reich, T.; Brendler, V.; Amayri, S.; Nitsche, H. Uranyl(VI) carbonate complex formation: Validation of the $Ca_2UO_2(CO_3)_{(3)}$(aq.) species. *Radiochim. Acta* **2001**, *89* (8), 511−518.
(45) Eliet, V.; Grenthe, I.; Bidoglio, G. Time-resolved laser-induced fluorescence of uranium(VI) hydroxo-complexes at different temperatures. *Appl. Spectrosc.* **2000**, *54* (1), 99−105.

Received for review December 14, 2005. Revised manuscript received April 24, 2006. Accepted May 30, 2006.

ES052507L